# Morphology, structures and properties of ZnO nanobelts fabricated by Zn-powder evaporation without catalyst at lower temperature

YUNHUA HUANG, JIAN HE
*Department of Materials Physics, University of Science and Technology Beijing, Beijing, 100083, China*

YUE ZHANG*
*Department of Materials Physics, University of Science and Technology Beijing, Beijing, 100083, China; State Key Laboratory for Advanced Metals and Materials, University of Science and Technology Beijing, Beijing 100083, China*
*E-mail: Yuezhang@ustb.edu.cn*

YING DAI, YOUSONG GU, SEN WANG, CHENG ZHOU
*Department of Materials Physics, University of Science and Technology Beijing, Beijing, 100083, China*

**Published online:** 28 March 2006

Uniform ZnO normal nanobelts and toothed-nanobelts have been successfully synthesized respectively through pure zinc powder evaporation without catalyst at 600°C. Experimental results indicate that the key to the fabricating method is to control the gas flow rates and the partial pressures of argon, oxygen and zinc vapor. Scanning electron microscopy and high-resolution transmission electron microscopy observations show that the ZnO nanobelts have several types of single crystalline morphology. HRTEM images reveal that there are numerous screw dislocations and the growth is around the dislocations in the toothed-nanobelts. The growth of ZnO nanobelts is controlled by vapor-solid and screw dislocation mechanisms. Room temperature photoluminescence spectra of the toothed-nanobelts showed a UV emission at ∼390 nm and a broad green emission with 4 subordinate peaks at 455–495 nm.


## 1. Introduction

Owing to the novel shapes, structures and properties, one (or quasi one) dimensional zinc oxide nanostructures have received considerable attention from the scientific community and achieved fruitful results. Besides nanowires, nanorods, nanorings, ZnO nanobelts and nanocombs have been fabricated and characterized [1, 2]. The crystal structure of zinc oxide nanomaterials is hexagonal with lattice constants of $a = 0.324$–$0.326$ nm and $c = 0.513$–$0.543$ nm. It has a wide band-gap of 3.37 eV and a large exciton binding energy of 60 meV at room temperature [3–5]. These properties make ZnO nanomaterials a good candidate for efficient room temperature excitonic laser. The chemical flexibility and the one-dimensionality of the nanomaterials make them ideal miniaturized laser light sources. These short-wavelength nanolasers could have myriad applications, including optical computing, information storage and microanalysis [6].

There are a series of methods for fabrication of 1D ZnO nanostructures. According to growth mechanism, the methods can be classified as vapor–liquid–solid (VLS) growth, vapor–solid (VS) growth and polar-surface dominated growth [2]. The VLS growth concerns the existence of a liquid (or so-called catalyst) phase [7]. Catalysts such as copper, gold, cobalt or other transition metal nanoparticles/films can often be used. In this method, the usual synthesizing temperature is in the range of 850–950°C [4–5, 7–9], and the lowest temperature for preparing ZnO

*Author to whom all correspondence should be addressed.
0022-2461 
DOI: 10.1007/s10853-006-6978-9

nanowires was reported as 450°C(NiO catalyzed) [10]. The temperature of synthesizing ZnO nanostructures by VS growth is between ~850°C (Zn-powder evaporation) to ~1400°C (zinc oxide powder evaporation) [11–17]. The temperature by VLS growth is much lower, but the catalysts in the nanomaterials will affect purity and possibly properties.

In this paper, we report an improved method to fabricate uniform nanobelts and toothed-nanobelts respectively onto silicon substrate by metal zinc powder evaporation and deposition without catalyst at the temperature of 600°C. The temperature was much lower than that in our previous work through a similar method [14–16]. We believed that our temperature was the lowest and the products were plentiful in the morphology while the fabrication contrasted with the reported ZnO nanobelts by VS growth. Numerous screw dislocations were observed in the toothed-nanobelts, and it was revealed that the growth was around the dislocations. The optical property of the ZnO toothed-nanobelts was also investigated by photoluminescence (PL) measurement at a room temperature.

## 2. Experimental procedures

The ZnO nanobelts were fabricated by the following procedure. The silicon substrate was placed face down on an alumina boat loaded with metal zinc powder (99.9%) with thickness of 1–3 mm. The vertical distance between the zinc source and the substrate was about 5–8 mm. The alumina boat was inserted into the quartz tube (30 mm inside diameter) of a tubular furnace under a constant flow of argon and oxygen. The total flow rate was 200–300 standard cubic centimeters per minute (sccm), and the fraction of oxygen was 1–5%. The quartz tube was heated up to 600°C, i. e. the reaction temperature, for 20–40 min. After the evaporation finished, the substrate surface showed white wax or fluffy-like materials. No catalyst was utilized in the deposition process.

The deposited products were characterized by scanning electron microscopy (SEM) [Cambridge S360], X-ray diffraction (XRD) [Rigaku DMAX-RB] and high-resolution transmission electron microscopy(HRTEM)[JEOL-2010]. The PL measurement was carried out on a HITACHI 4500-type Vis-UV spectrophotometer with a Xe lamp as the excitation light source at room temperature.

## 3. Results and discussion

High yield ZnO nanobelts were fabricated by controlling the flow rates and partial pressures of argon, oxygen and Zn vapor at the temperature of 600°C. The shapes of ZnO belts were changed with growth condition. The fabricated belts exhibited several kinds of shapes, i. e. normal belts (as seen in Fig. 1a synthesized at Ar $+ O_2$ (1–2%) = 280–300 sccm) and diverse toothed-nanobelts (as seen in Fig. 1b, Ar $+ O_2$ (1–2%) = 250–270 sccm; Fig. 1c, Ar $+ O_2$ ( ~2%) = 200–230 sccm; Fig. 1d, Ar $+ O_2$ (3–5%) = 220–260 sccm). The typical width of the belts is about 400 nm to 900 nm, the thickness is around 10–50 nm, while the length of the belts is up to several tens of microns. The teeth of the toothed-belts have diameters ranging from 10–100 nm and lengths are tens of nanometers to hundreds of nanometers. Some of the teeth are thinner than the backbones, such as Fig. 1b; some have the same thickness as the backbones, as seen in Fig. 1c; and others are thicker than the backbones, and backbones are not uniform in thickness, such as seen in Fig. 1d.

In our experiments, ZnO nanobelts were fabricated through Zn-powder evaporation without catalyst at lower temperature. The main parameters fabricating method are to control the gases flow rates, partial pressures of argon, oxygen and zinc vapor. The flow rates and partial pressures of argon and oxygen influence the size of nanostructures, and more importantly determine the shape (belts with or without teeth). Experiments revealed that the synthesis temperature influences the shapes by changing the partial pressures of Zn, and also affects the size. The nanostructures prefer being toothed-belts to entire belts and the sizes become larger as the temperature or partial pressure of Zn vapor increases at constant flow of argon and oxygen. Also it becomes more difficult to control the shape of nanobelts as the temperature increases. The nanostructures with smaller length to diameter ratio, belts with teeth, and larger size form readily at the areas where the gas flow is blocked, or when the gas flow rate decreases. The effects of partial pressure of vapor phase are more complicated and sensitive than flow rates of gases. Generally, toothed-structures are easier to grow as the partial pressure of $O_2$ increases. But it need further study to determine the synergetic effect of partial pressure and gas flow.

Fig. 2 show the TEM and HRTEM images, selected area electron diffraction (SAED) pattern of a toothed-belt, screw dislocations and the growth steps in the tooth are also showed. SAED pattern and HRTEM images reveal that the ZnO toothed-nanobelts are structurally uniform and single crystalline. HRTEM images also show numerous screw dislocations in the tooth. The arrowheads indicate some place of dislocations in Fig. 2a and the high resolution local images are shown in Fig. 2c and d. The images exhibit periodic dislocations and the growth steps. The growth is around the dislocations, and the growth direction accords with the Burgers vector of the dislocations. Fig. 2a and b suggested that the tooth growth occurs along the [0001] direction. But some others grow along the [$2\bar{1}\bar{1}0$] direction in our observations. The results showed that the teeth of such belts may orientated in "c" or "a" direction. In the same way, backbones of the toothed-belts may grow in "a" or "c" direction accordingly.

XRD measurements were made on all the fabricated nanostructures to assess the structure and phase purity. The investigations show that all the deposited nanostrctures on the silicon substrate are pure ZnO with hexagonal wurtzite structure. No diffraction peaks from Zn or other impurities were found in our sample. The diffraction peaks

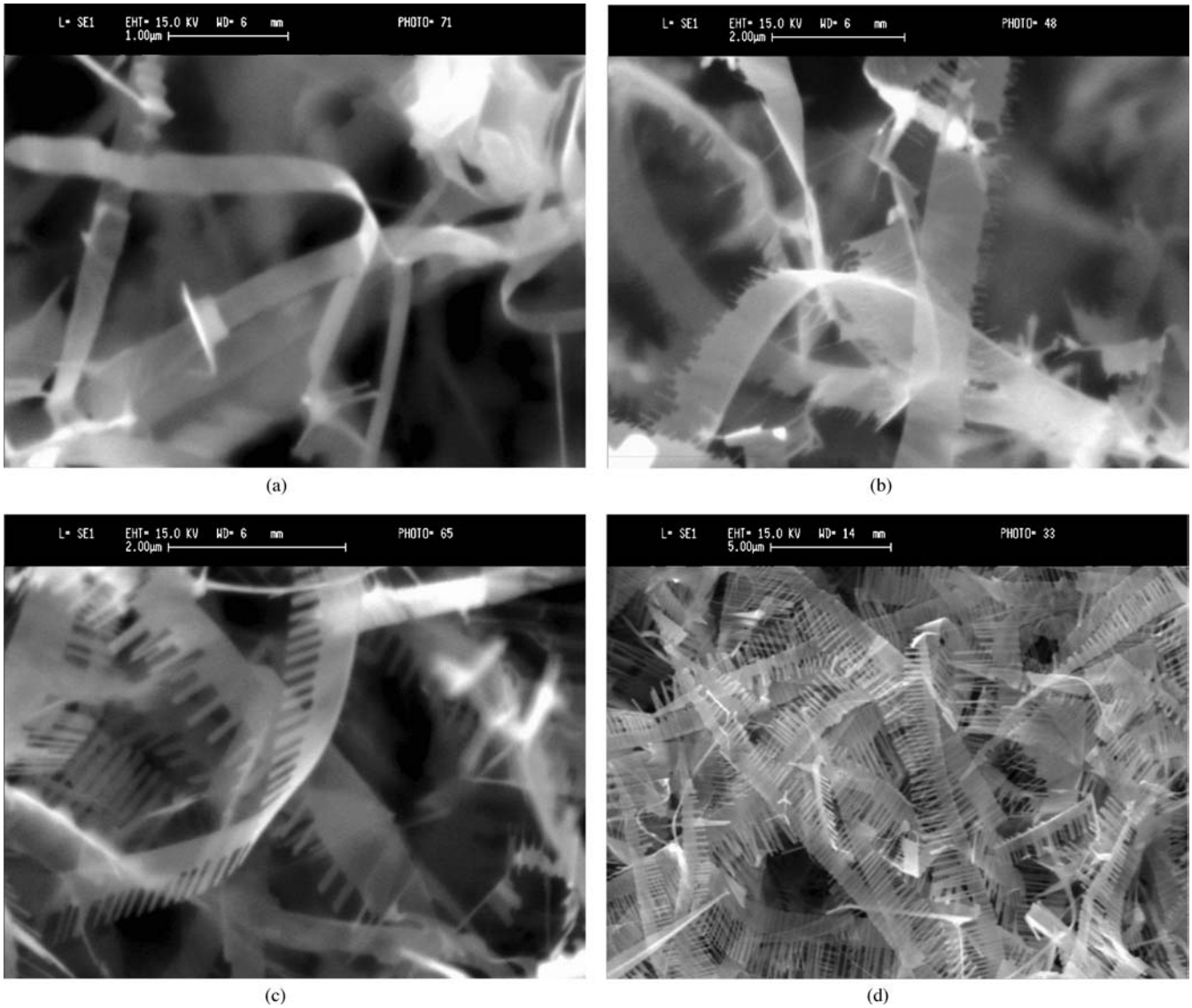


*Figure 1* SEM images of ZnO nanobelts (a. Normal nanobelts; b. c. d. Toothed-nanobelts).

can be indexed to a wurtzite structure of ZnO with cell constants of $a = 0.3242$ nm and $c = 0.5194$ nm. Fig. 3 shows the XRD spectra of the toothed-nanobelts and the indexed results.

Conventionally, there are several possible models for the growth of crystal whisker, VLS [18], VS [19] and screw dislocation [20]. VLS [4, 7, 8], VS [12, 15] and screw dislocation [21] mechanisms are applied successfully to the growth of 1D nanomaterials. For example, Zhang et al. discussed the screw-dislocation-induced growth mechanism in helical crystalline silicon carbide nanowires covered with a silicon oxide sheath ($SiC/SiO_2$) [21]. But so far, the screw dislocation has not been confirmed in 1D ZnO nanostructures. The solidified spherical droplets at the tips of the nanowires or others are commonly considered to be the evidence for the operation of the VLS mechanism [7]. But nothing except ZnO was found at the HRTEM image around the tip of tooth. This agrees with the result of XRD. The results deny the VLS growth, but confirm VS growth in our fabrication. On the other hand, HRTEM micrograph analysis is credible to confirm dislocation and growth of crystal whisker [22]. In the same way, HRTEM analysis confirmed screw dislocation in the toothed-belts. In a word, the above investigations indicate that the growth of ZnO nanobelts is controlled by the screw dislocation and VS mechanisms.

PL spectrum of ZnO toothed-nanobelts (Fig. 1d) at room temperature was measured and shown in Fig. 4. The excited wavelength was 310 nm. Two typical emission peaks at ~390 nm and at 455–495 nm were observed, which was assigned to the UV emission and green emission, respectively. It was difficult to observe UV light emission from bulk ZnO at ambient temperature. Bagnall et al. [23] demonstrated that the improvement of crystal quality (decrease of impurities and structure defects) can result in detectable UV emission at room temperature. Vanheusden et al. [24] proved that the green transition has been attributed to the singly ionized oxygen vacancy

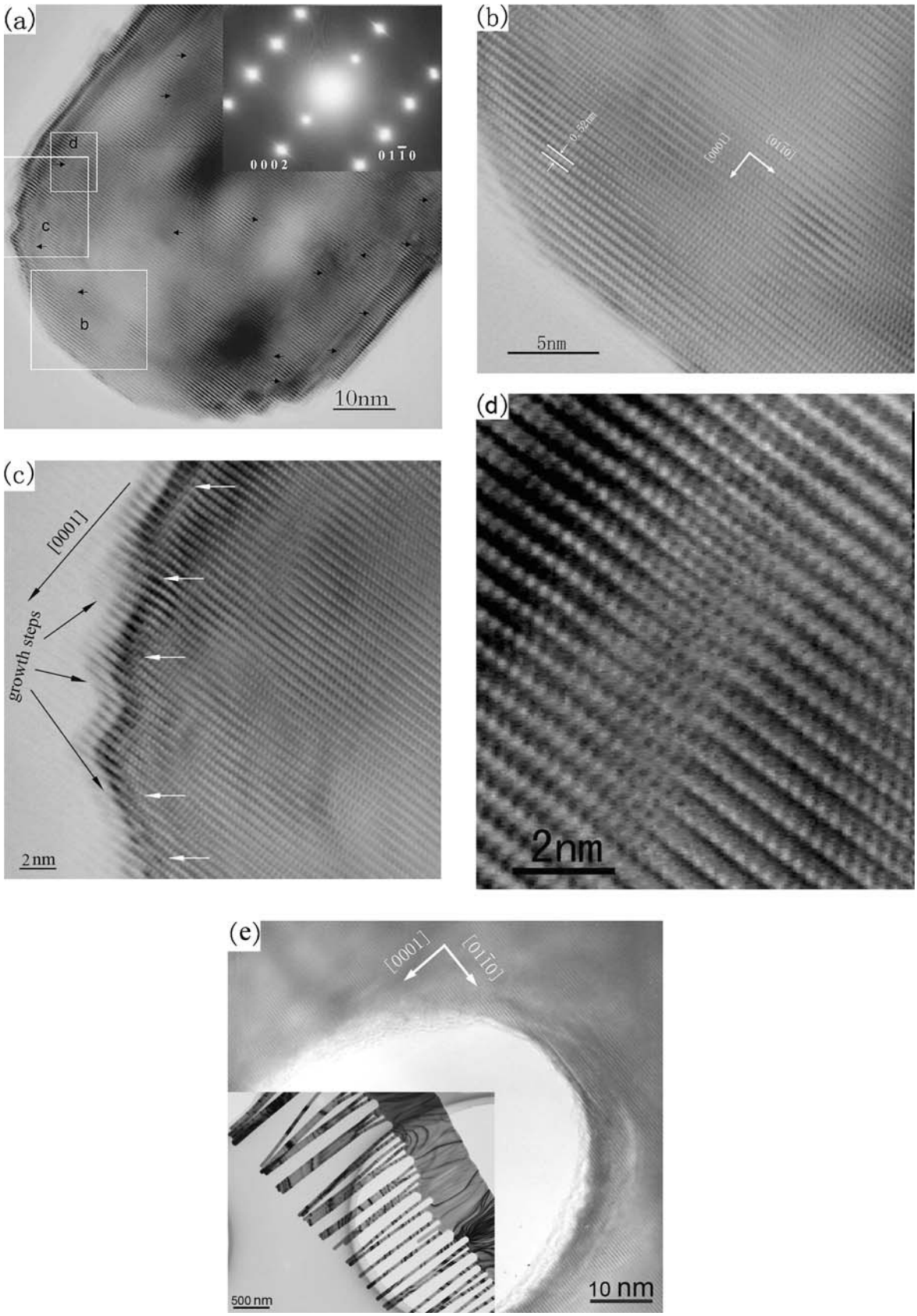


*Figure 2* a. HRTEM image and SAED pattern of the tooth of ZnO toothed-nanobelt (the arrowheads point out the positions of dislocations and the white rectangles show the areas magnified in latter figures); b. HRTEM image (higher magnification of "b" area in a); c. Screw dislocations and growth steps (higher magnification of "c" area in a; the white arrowheads point out some positions of dislocations); d. Screw dislocations (higher magnification of "d" area in a); e. TEM and HRTEM images of the nanobelts and the joint of tooth and backbone.

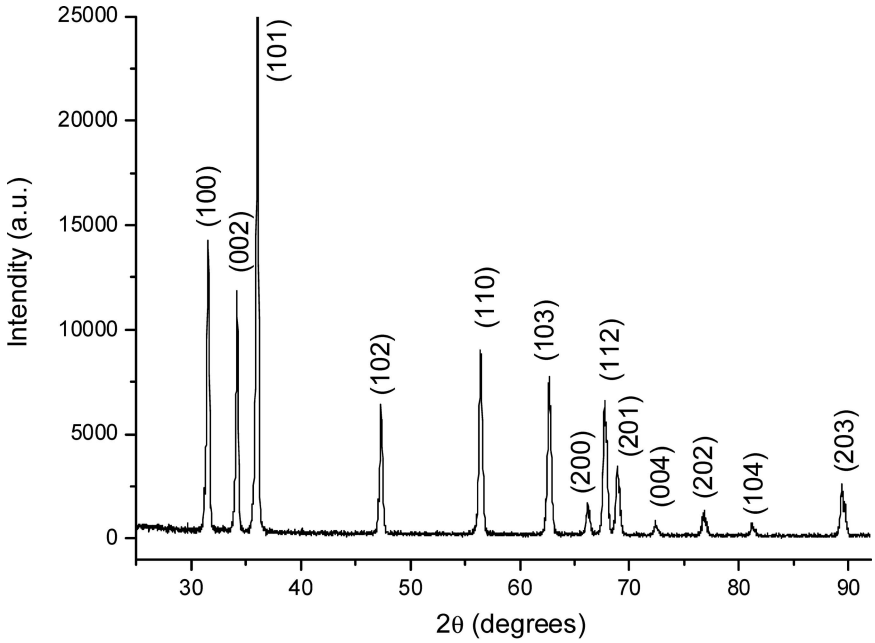


*Figure 3*. XRD pattern of ZnO toothed-nanobelts.

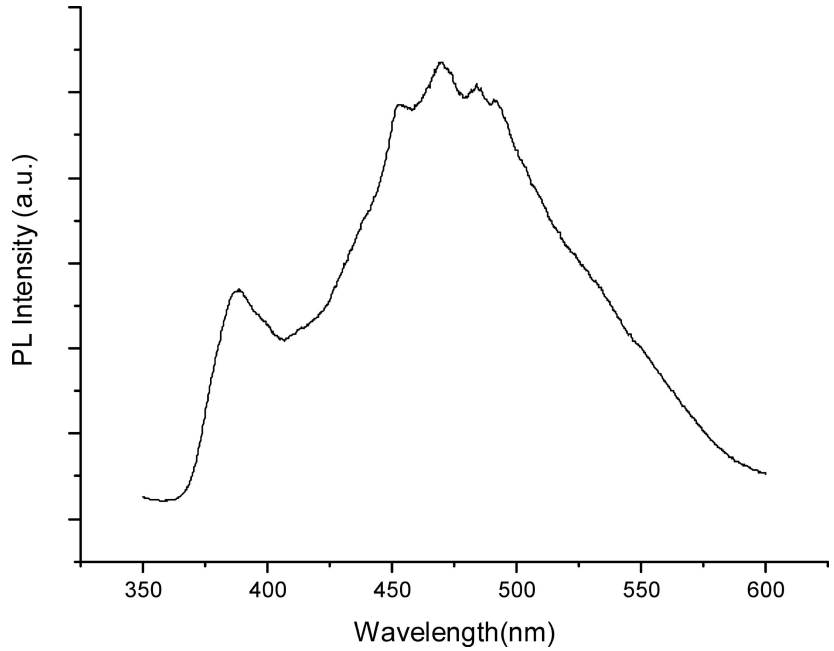


*Figure 4*. Photoluminescence spectrum of ZnO toothed-nanobelts at room temperature.

in the ZnO and the emission results from the radiative recombination of a photogenerated hole with an electron occupying the oxygen vacancy. Huang et al. [25] reported that the green light emission intensity increases relative to the UV emission as the wire diameter decreases, which suggested that there is a great fraction of oxygen vacancies in the thinner nanowires. Therefore, it is reasonable to believe that there exist some oxygen vacancies in the ZnO toothed-nanobelts and the green light emission from the ZnO toothed-nanobelts could be attributed to the single ionized oxygen vacancy.

Specially, the emission peak at 455–495 nm includes 4 subordinate peaks. We consider that it results from the combination of PL spectra with different peak values. PL peak position can be changed along with the type or quantity of oxygen vacancies which are affected by the dimension of ZnO nanostructures. Z.L.Wang et al.[26] reported the excursion of PL spectra of ZnO nanobelts with different dimension and confirmed such size effect. Therefore, subordinate peaks are produced essentially by size effect of ZnO nanostructures.

## 4. Conclusions

We have successfully synthesized ZnO normal nanobelts and toothed-nanobelts by Zn-powder evaporation without catalyst at 600°C. The temperature is far lower than the other reported temperature of synthesizing ZnO nanostructures by VS growth. The key parameters of the fabricating method are the gases flow rates, partial pressures of argon, oxygen and zinc vapor. The synthesis temperature, gases flow rates and vapor partial pressures determine the shape and size of the ZnO nanostructures. SEM and HRTEM observations show that the ZnO nanobelts have several types of morphology, and all of them are single crystalline. Also, the HRTEM images reveal that there are numerous screw dislocations and the growth is around the dislocations in the toothed-nanobelts. The growth of ZnO nanobelts is controlled by VS and screw dislocation mechanisms. Room temperature PL spectra of the toothed-nanobelts showed a UV emission at ~390 nm and a broad green emission at 455–495 nm with 4 subordinate peaks.


## Acknowledgements

This work was supported by the National Science Fund for Distinguished Young Scholars (No. 50325209), the National Natural Science Foundation of China (No. 50232030, 50572005) and the Key Project of Chinese Ministry of Education (104022).


## References


1. Z. W. PAN, Z. DAI and Z. L. WANG, *Sci.* **209** (2001) 1947.
2. Z. L. WANG, X. Y. KONG and J. M. ZUO, *Phys. Rev. Lett.* **91** (2003) 185502.
3. C. J. LEE, T. J. LEE, S. C. LYU and Y. ZHANG, *App. Phys. Lett.* **81** (2002) 3648.
4. S. Y. LI, C. Y. LEE and T. Y. TSENG, *J. Cryst. Growth* **249** (2003) 201.
5. H. J. YUAN, S. S. XIE, D. F. LIU, X. Q. YAN, Z. P. ZHOU, L. J. CI, J. X. WANG , Y. GAO, L. SONG and L. F. LIU, *Chem. Phys. Lett.* **371** (2003) 337.
6. M. H. HUANG, S. MAO, H. FEICK, H. YAN, Y. WU, H. KIND, E. WEBER, R. RUSSO and P. YANG, *Sci.* **292** (2001) 1897.
7. Y. W. WANG, L. D. ZHANG, G. Z. WANG, X. S. PENG, Z. Q. CHU and C. H. LIANG, *J. Cryst. Growth* **234** (2002) 171.
8. P. YANG, H. YAN, S. MAO, R. RUSSO, J. JOHNSON, R. SAYKALLY, N. MORRIS, J. PHAM, R. HE and H. J. CHOI, *Adv. Func. Mater.* **12** (2002) 323.
9. H. YAN, R. HE, J. PHAM, and P. D. YANG, *Adv. Mater.* **15** (2003) 402.
10. S. C. LYU, Y. ZHANG, H. RUH, H. J. LEE, H. W. SHIM, E. K. SUH and C. J. LEE, *Chem. Phys. Lett.* **363** (2002) 134.
11. J. S. LEE, M. I. KANGA, S. KIM, M. S. LEE and Y. K. LEE, *J. Cryst. Growth* **249** (2003) 201.
12. Z. R. DAI, Z. W. PAN and Z. L. WANG, *Adv. Func. Mater.* **13** (2003) 9.
13. X. Y. KONG, Y. DING, R. S. YANG and Z. L. WANG, *Sci.* **303** (2004) 1348.
14. Y. DAI, Y. ZHANG and Z. L. WANG, *Solid State Commun.* **126** (2003) 629.
15. Y. DAI, Y. ZHANG, Q. K. LI and C. W. NAN, *Chem. Phys. Lett.* **358** (2002) 83.
16. Y. DAI, Y. ZHANG, Y. Q. BAI and Z. L. WANG, *Chem. Phys. Lett.* **375** (2003) 96.
17. J. Y. LAO, J. Y. HUANG, D. Z. WANG and Z. F. REN, *Nano Lett.* **3** (2003) 235.
18. R. S. WAGNER and W. C. ELLIS, *Appl. Phys. Lett.* **4** (1964) 89
19. H. M. JENNING and J. MATER. *Sci.* **18** (1983) 951
20. J. DONG, W. SHEN, B. ZHANG, X. LIU, F. KANG, J. GU, D. LI and N. CHEN, *Carbon*, **39** (2001) 2325
21. H. F. ZHANG, C. M. WANG and L. S. WANG, *Nano Lett.* **2** (2002) 941.
22. K. C. HUNG, C. C. LAM, J. Q. LI and H. M. SHAO, *Phys. C* **28**2–2**87** (1997) 907.
23. D. M. BAGNALL, Y. F. CHEN, M. Y. SHEN, Z. ZHU and T. YAO, *J. Cryst. Growth* **185** (1998) 605.
24. K. VANHEUSDEN, W. L. WARREN, C. H. SEAGER, D. R. TALLANT, J. A. VOIGT and B. E. GNADE, *Appl. Phys.* **79** (1996) 7983.
25. M. H. HUANG, Y. WU, H. FEICK, N. TRAN, E. WEBER and P. D. YANG, *Adv. Mater.* **13** (2001) 113.
26. X. WANG, Y. DING, C. J. SUMMERS and Z. L. WANG, *J. Phys. Chem. B* **108** (2004) 8773.



*Received 5 March*
*and accepted 13 September 2005*